# Evidence for thermalization of surface-desorbed molecules at heating rates of $10^8$ K/s

C. R. Maechling,[a] S. J. Clemett, F. Engelke,[b] and R. N. Zare
*Department of Chemistry, Stanford University, Stanford, California 94305*

(Received 12 September 1995; accepted 27 February 1996)

Laser desorption of aniline-*d*7 from a single-crystal surface (0001) of sapphire ($Al_2O_3$) at a heating rate on the order of $10^8$ K/s was studied using pulsed infrared laser radiation for desorption and resonance enhanced multiphoton ionization (REMPI) for detection of the desorbed aniline molecules. On the basis of single-vibronic-level fluorescence (SVLF) spectra we unambigiously assign the 10*b* transition. REMPI spectroscopy provides vibrational temperatures and therefore describes the internal energy distribution, whereas the time-of-flight (TOF) profiles provide translational temperatures. All results are consistent with a thermal mechanism for desorption, i.e., pulsed heating of the sapphire surface on the nanosecond time scale leads to thermal desorption and rapid thermalization of the escaping molecules. © *1996 American Institute of Physics.* [S0021-9606(96)01121-X]

## I. INTRODUCTION

Laser desorption (LD) is an effective method for volatilizing large, polar, and nonvolatile molecules intact as opposed to traditional heating methods that can cause decomposition.[1,2] Perhaps the best demonstration of its utility has been in the analysis of fragile biomolecules; proteins as large as 450 000 amu have been volatilized with LD.[3] Owing to the great variety in wavelengths, temporal widths, and energies of pulsed laser sources, the mechanism of LD cannot be satisfactorily described by only one mechanism. Additionally, the composition of desorption substrates (metals, semiconductors, insulators, or matrix molecules) complicates the description of the mechanism responsible for the desorption event.

Depending on the wavelength of the laser, LD can be performed directly via resonant excitation of vibrational modes or electronic states of the adsorbates or indirectly via heating of the substrate or surrounding matrix. The former is known as resonant laser desorption and the latter is known as laser-induced thermal desorption. Resonant laser desorption involving infrared (ir) excitation of vibrational modes of adsorbates[4–7] and the ultraviolet (uv) excitation of electronic states of adsorbates[8,9] have been performed on a variety of systems. Although resonant uv laser desorption can be used for the selective desorption of molecular species from mixtures,[8] resonant ir laser desorption has failed in this task. Chuang[4] and Heidberg and Hoge[6] found that intermolecular coupling and surface heating effects from adsorbate–surface coupling prevent the observation of selective desorption of mixtures. Infrared laser desorption is therefore exclusively a nonresonant effect.

Our experiments are designed to heat directly the surface and do not involve the resonant excitation of adsorbates. This paper describes our approach to unraveling the mechanism of the pulsed ir laser-induced desorption of molecules from a dielectric surface. We have conducted experiments to investigate the equilibrium nature of the laser-induced thermal desorption process by monitoring the flow of energy from a laser-heated substrate into polyatomic molecules adsorbed to the surface of the substrate. We have studied the system of aniline ($C_6H_5NH_2$, 93.0577 amu) and aniline-*d*7 ($C_6D_5ND_2$, 100.1018 amu) adsorbed to the single-crystal surface (0001) of sapphire ($Al_2O_3$). Aniline is an excellent probe molecule because its resonance enhanced two-photon laser ionization (REMPI) spectroscopy is accessible with simple laser dye mixtures.[9–13] Sapphire is an ideal insulator surface because it can be superpolished[14] to a very uniform flat surface and maintains a chemically homogeneous surface of hydroxyl groups.[15]

Laser-induced thermal desorption has numerous applications and has been extensively studied;[16] however, few studies have explored the transfer of energy as desorbed molecules make the transition from surface-bound to gas-phase species. Voumard *et al.*[17,18] and Elokhin *et al.*[19] have demonstrated that internal energy resolved detection of desorbing molecules is a powerful tool for elucidating the laser-induced thermal desorption mechanism. Voumard *et al.*[17,18] have studied the mechanism responsible for intact volatilization of aniline from a quartz surface. They report that aniline molecules leave the dielectric surface with internal energies of $360\pm60$ K for the vibrational states and $350\pm100$ K for the rotational contours, well below that of the calculated surface temperature of 500 to 600 K. Their results support a desorption mechanism dominated by a bottleneck in the energy flow from the surface into the adsorbates during laser-induced thermal desorption. Elokhin *et al.*[19] have investigated the system of aniline desorption from a stainless steel surface. They find that many layers of aniline desorbed from the surface with a vibrational energy of $420\pm40$ K; however, mixtures of aniline and carbon dioxide desorb with an internal energy of $170\pm30$ K. They conclude that the aniline is collisionally cooled, similar to a supersonic expansion, when

[a]Present address: Booz·Allen & Hamilton, 225 West Wacker Dr., Chicago, IL 60606.
[b]Permanent address: FHF, D-78116 Furtwangen/Schwarzwald, Germany.

 0021-9606/96/104(21)/8768/9/$10.00 

desorbed in combination with carbon dioxide.

To follow the energy transfer processes we (1) monitor the time dependence of the surface temperature upon laser heating, (2) measure the translational and internal energy distributions of desorbed molecules using two-step laser mass spectrometry ($L^2MS$), and (3) compare the two energy distributions with each other and the surface temperature profile to determine if the molecules are in thermal equilibrium with the surface at the time of desorption.

## II. LASER-INDUCED THERMAL DESORPTION

The mechanism of desorption from a heated substrate can be described unambiguously;[20] however, unique features arise when short laser pulses are used to create an extremely rapid heating event. Short laser pulses are absorbed by vibrational modes or valence electrons at the surface of a substrate, and the energy of the laser pulse is rapidly converted into thermal energy. Unlike the resistive heating rates typically used in temperature programmed desorption studies ($10^0$–$10^3$ K/s), pulsed laser excitation can be used to create a rapid ($10^6$–$10^{12}$ K/s) short-time heating of surfaces. Coincidentally, a thermal desorption mechanism is employed to describe fast particle bombardment techniques like plasma desorption mass spectrometry, secondary ionization mass spectrometry, and fast atom bombardment. In these methods, the heating rates of the substrates are determined by the impulsive energy of the particle and the stopping power of the surface.[21]

One difference between the desorption of molecules from slowly and rapidly heated gas–surface systems is the density of molecules leaving the surface per unit time. For laser desorption, the flux of molecules leaving the surface can be large and a significant number of collisions may occur before detection; the role of collisions must carefully be considered. Kelly and Dreyfus[22] have seen that with a pulsed laser heating source a tendency exists for near-surface collisions to occur, and as few as three collisions per particle already lead to Knudsen layer effects in time-of-flight (TOF) measurements. Additionally, NoorBatcha *et al.*[23] have performed a direct Monte Carlo approach. They found that post-desorption collisions of molecules desorbed under thermal conditions from coverages of greater than 0.1 monolayers (ML) altered the velocity distributions. For inelastic collisions, the altered velocity distributions have the form of a Maxwellian velocity distribution that includes a stream velocity. Internal energy distributions have been used by Asscher *et al.*[24] to probe the equilibrium nature of the desorption mechanism. These distributions are especially important to understanding the desorption mechanism because translational energy distributions can be obscured by interferences from collisions and cooling resulting from interactions with the surface past the transition state, i.e., from an exit barrier.

Laser-induced desorption has been treated as thermal desorption on a very rapid time scale. This treatment, however, does not explain the observation that thermally labile, polar, and nonvolatile compounds can be desorbed without fragmentation at high heating rates while decomposing at low heating rates.[1] Preferential intact desorption by rapid heating can be explained with a competitive kinetic model, whereby the rate of desorption greatly exceeds the rate of decomposition. This behavior requires that the system (substrate–adsorbate) be in complete equilibrium and adsorbates leave the surface with an energy, both translational and internal, equivalent to the surface temperature.

Zare and Levine[25] have proposed an alternative model of bond-selective processes in rapid desorption based upon the nonequilibrium nature of the system. In this scenario, the adsorbate comes off the surface vibrationally ''cold'' because equilibrium with the substrate is never achieved owing to a bottleneck in the transfer of the energy from the surface to the adsorbate. They argue that energy can flow between phonon modes of the substrate and the adsorbate–surface physisorption bond, as these are appropriately matched low-frequency oscillators, but a mismatch between frequencies of the physisorption bond and the internal modes of the adsorbate allows the adsorbate to desorb before appreciable energy can flow into the adsorbate and cause decomposition. Unlike physisorbed systems, chemisorbed systems are not as accurately described by this model because the coupling between the various modes is stronger. Holme and Levine[26] have modeled the desorption processes initiated by rapid surface heating with classical molecular dynamics simulations. Their simulations show that bottlenecks are possible for physisorbed diatomics; however, energy was equipartitioned for more strongly bound, chemisorbed, systems. Lucchese and Tully[27] have studied laser-induced desorption of physisorbed systems using a generalized Langevin method and observed that rapid heating rates allowed molecules to desorb with energies below the corresponding surface temperature.

Although some work has appeared on the effects of collisions in the desorption process,[23] most theoretical simulations of desorption are performed on a molecule-by-molecule basis and omit collisional effects. Another mechanism that can explain how laser desorption volatilizes fragile molecules intact is post-desorption collisional cooling, where large numbers of collisions internally cool the desorbed molecules. Experimental confirmation of low plume temperatures has been observed using labile molecules as ''thermometers'' in matrix-assisted laser desorption ionization (MALDI) experiments.[16]

## III. EXPERIMENT

A schematic of the apparatus is depicted in Fig. 1 and a full description may be found elsewhere.[28] The experiments are performed in an UHV chamber which has an operating pressure of $3\times10^{-9}$ Torr. Single-crystal sapphire with a diameter of 5.08 cm and a thickness of 0.1 cm is mounted at the bottom of a liquid-nitrogen-cooled cryostat on a differentially pumped rotable feed through. After cleaning with acetone and methanol, the sapphire sample is cleaned in vacuum by exposure to high energy pulses of the ir laser.

Aniline is dosed onto the surface using a glass microcapillary array (0.6 cm diam.) positioned 0.3 cm above the surface. The assembly is positioned such that the $L^2MS$ experi-

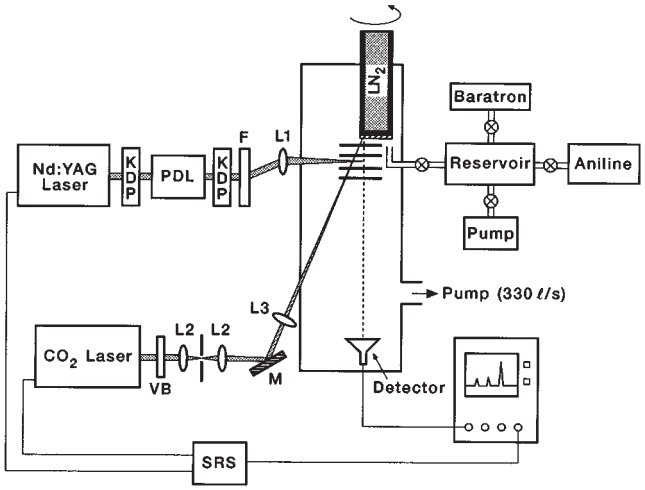


FIG. 1. Schematic of the apparatus used to study the ir laser-induced-thermal desorption mechanism. Some abbreviations are F=filter, L=lenses, $LN_2$=liquid nitrogen, M=gold mirror, PDL=pulsed dye laser, SRS=pulse generator, VB=Venetian blind.

ments are carried out on one side (above the ion source) while the surface is being repopulated with fresh analyte from a gas reservoir on the other (above the gas doser). The surface is carefully mounted so that the surface normal is colinear with the axis of rotation of the dewar assembly.

The $TEM_{00}$ output of a pulsed ir laser ($CO_2$, Alltec AL-851, 10.6 $\mu$m) is focused with a ZnSe lens (25 cm focal length) onto the adsorbate-covered surface and causes rapid desorption of neutral molecules from a spot size of roughly 1 mm in diameter. Infrared laser attenuation is performed with a variable high-power spatial filter/attenuator similar to one described by Bialkowski.[29] After a prescribed time delay, the doubled output of a dye laser (Quanta-Ray PDL-1) pumped by a Nd:YAG laser (Quanta-Ray DCR-11, 532 mm) ionizes the desorbed species by (1+1) REMPI. The ionization laser is focused with a cylindrical lens (35 cm focal length) into a ribbon that passes between the extraction electrodes. The beam waist along the axis of the TOF axis is $\sim$250 $\mu$m and the confocal parameter is 2.5 cm. The power of the ionization laser is kept low enough to avoid saturation effects.

Surface coverages are estimated as follows: One monolayer is defined as being equivalent to the surface density of close-packed aniline molecules lying flat on a surfce. Estimating the dimensions of aniline to be 5.5 Å$\times$7 Å, we calculate that a monolayer is composed of $2.6\times10^{14}$ molecules/cm$^2$. For one rotation of the surface, a 17 cm$^2$ ring is dosed with aniline. Assuming a sticking coefficient of aniline to the cold sapphire surface to be unity, an upper limit of the surface coverage in monolayers can be calculated from the amount of aniline leaked into the chamber and the rotation speed of the sapphire surface. Using a fixed surface rotation rate of 0.8 rev/min the coverage is a function only of leak rate. The leak rate is determined by measuring the pressure of the reservoir using a very accurate (to $10^{-5}$ Torr) capacitance manometer (MKS Baratron 390); the number of molecules leaving the reservoir is estimated from the pressure decrease using the ideal gas law. By adjusting the leak valve between the reservoir and the system, we control the coverages of aniline deposited onto the surface. We calculate an upper limit of coverage to be $\sim$0.15 ML for our submonolayer studies and $\sim$1.5 ML for our monolayer studies. In addition, we have observed that for dosing up to monolayer coverages the intensity of scattered aniline molecules is almost zero, which supports the assumption that the sticking coefficient of aniline on sapphire is close to unity.

Aniline-*d*7 is used not because it is chemically more interesting than other moderate-sized polyatomics, but rather because the spectroscopy of aniline is manageable[9,10,12,13] and the dye laser system needed to perform (1+1) REMPI is simple to operate.

Our TOF mass spectrometer is equipped with a two-stage Wiley–McLaren source.[30] The ir laser pulse desorbs molecules from the surface after passing through electroformed mesh-covered holes in the extraction electrodes. The desorbed neutral plume enters the extraction region (first stage) of the ion source, and ions are created by (1+1) REMPI at the center of this stage. A small hole (1 mm) in the plate that separates the extraction region from the acceleration region (second stage) allows only that fraction of the plume having velocity components normal to the surface to pass through and thus be detected by the microchannel plate assembly. By selecting only normal velocity components, the contributions from angular distribution of desorbing species are removed. This velocity component selection greatly simplifies our data analysis.

The geometry of the extraction stage is very constricted and additional plates are included to maintain uniform fields. Similarly, several plates are included after the acceleration region to prevent field distortions that the ions might experience before reaching the grounded TOF drift tube (5.08 cm diameter, 1 m long). Voltages are supplied to three of the plates from power supplies external to the chamber, and resistors are attached to the other plates to provide uniform field gradients. Following the mathematical treatment of a TOF mass spectrometer equipped with a two-stage ion source,[30] we selected the voltages and distances between plates to provide optimal mass resolution, approximately 350.

The ions are mass analyzed with a TOF mass spectrometer and detected with dual microchannel plates in a chevron configuration. The signal is amplified with a fast preamplifier (Ortec 9301, $\times$10) and recorded with a digital storage oscilloscope (LeCroy 9450, 350 MHz). A pulse generator is used to control the timing of the two lasers and the data acquisition.

Data acquisition is divided into two types of experiments: (1) gas phase and (2) two step. Gas-phase experiments, such as acquiring a REMPI spectrum or calibrating the vibrational spectroscopy, were performed using a ''summed averaging'' program provided with the oscilloscope. Summed averaging consists of the repeated addition, with equal weight, of successive source waveform records. A computer is used to scan the dye laser to different wavelengths, and the averaged spectra are transferred from the

oscilloscope and saved to disk as files corresponding to laser frequency. Averaged spectra are recorded at the uv laser repetition rate of 10 Hz.

Two-step experiments are controlled differently because the ir laser cannot produce a stable output of pulses at repetition rates greater than 5 Hz and the uv laser produces a stable output of pulses at a rate of 10 Hz. The ir laser is triggered by a divide-by-two circuit to circumvent this repetition rate mismatch. Both lasers, therefore, are operated at maximum stability. The oscilloscope is operated in ''sequence mode'' and triggered at 10 Hz. Sequence mode involves the scope saving each spectrum and building a trace of many contiguous mass spectra. A trace is composed of alternating types of spectra; a spectrum arising from a two-step event followed by one arising from a purely gas-phase event (i.e., background). Proper steps are taken to identify which spectrum corresponds with which event. A sequenced trace is transferred to a computer, divided, and the pieces recombined to form two files of an averaged spectra—one of two-step signal and one of gas-phase signal. The averaged gas-phase signal is subtracted from the averaged two-step signal to create a background-corrected two-step signal.

The energy transfer from a surface to adsorbates can be monitored by measuring (1) the time dependence of the surface temperature, (2) the translational energy distributions of the desorbed molecules, and (3) the internal energy distributions of the desorbed molecules. Measurement (1) has been performed on a quartz surface that was rapidly heated using a pulsed ir laser,[31] and was successfully (within 10%) simulated using a finite difference model of the heat conduction equation.[32] Measurement (2) is performed by measuring signal (at a fixed ionization laser wavelength) as a function of time delay between the desorption laser pulse and the ionization laser pulse. Because the distance from the surface to the ionization region is fixed, this technique allows us to record a profile of the molecules leaving the surface; we refer to this technique as time-of-flight profiling. TOF profiles, i.e., velocity distributions, are recorded by varying the delay times in a pattern whereby adjacent time delay values are never recorded back-to-back in time. By determining delay times in this alternating fashion, our TOF profiles, when smooth, indicate that no systematic errors are introduced during the course of an experiment. Measurement (3) is performed by recording signal (at a fixed time delay between desorption and ionization pulses) as a function of ionization wavelength. Because the ionization laser can be tuned to produce $(1+1)$ REMPI from various vibrational levels of the electronic ground state of the desorbing molecules, we can derive the vibrational populations of desorbing molecules from the signal strengths by correcting for the different absorption transition probabilities.

## IV. RESULTS

Numerical calculations of pulsed ir laser heating of a sapphire substrate suggest that we are performing laser-induced thermal desorption with a surface heating rate on the order of $10^8$ K/s (Sec. IV A). TOF profiles are compared with Maxwell–Boltzmann distribution functions to determine the translational energy of the desorbing aniline (Sec. IV B). On the basis of single-vibronic-level fluorescence (SLVF) spectra we assign the $T_1^1$ transition to the $10b_1^1$; previous assignments of this transition were ambiguous (Sec. IV C). The $10b_1^1$ transition and the origin transition are used to determine the vibrational energy of the desorbing aniline (Sec. IV D). Our results indicate that aniline molecules desorbing from a sapphire surface at a heating rate of $10^8$ K/s with a translational energy of approximately 400 K and an internal, vibrational, temperature of 415 K.

### A. Surface temperature

Previously in this laboratory, the surface temperature-time profile of fused quartz irradiated by a ir laser pulse was simulated using a finite difference model of the heat conduction equation,[32] and good quantitative agreement was obtained with profiles measured experimentally using a platinum resistance thermometer adhered to the fused quartz substrate.[31] This simulation has been rewritten to include a temporal profile of our ir laser with the temperature-dependent thermal parameters and an optical parameter characteristic of sapphire.[33] The radiation penetration depth is estimated from the optical absorption coefficient used in the simulations to be $\sim 4$ $\mu$m (the radiation penetration depth is simply the reciprocal of the absorption coefficient). This value of radiation penetration depth satisfies that the laser pulse is absorbed in the top layer of the sapphire, creating a rapid heating event at the surface. The heat diffusion length is strictly a function of the thermal parameters and the duration of the laser pulse, and calculations for temperatures up to 2000 K show that this length is never larger than 50 $\mu$m. Because the laser spot size is 1 mm, much larger than the thermal diffusion length, a one-dimensional treatment of the heat conduction equation is used to describe the temperature at the center of the laser spot. We believe that this simulation provides accurate temperature-time profiles (at least to within 10% as was seen in the quartz studies). Three user-defined inputs can be adjusted (pulse energy, layer thickness, and time interval) to produce surface temperature profiles.

From the simulations, we find that sapphire is very much like quartz in its surface temperature response to ir laser (10.6 $\mu$m) pulses. For a typical pulse energy, we calculate heating rates on the order of $10^8$ K/s, and a peak surface temperature of 1000 K. Because the low-frequency phononic modes of the substrate can efficiently couple energy into the adbond, the temperature of the surface is equivalent to the temperature of the adbond. Therefore, a more accurate method of describing the surface temperature, at least at the time of desorption, is found in the time-of-flight profiles (a measure of the energy of the surface–adsorbate bond) of the desorbing molecules.

### B. Translational energy distributions

Translational energy distributions were studied for submonolayer and monolayer coverages using both the $O_0^0$ and the $10b_1^1$(see Sec. IV 3C) transitions. The TOF profiles for

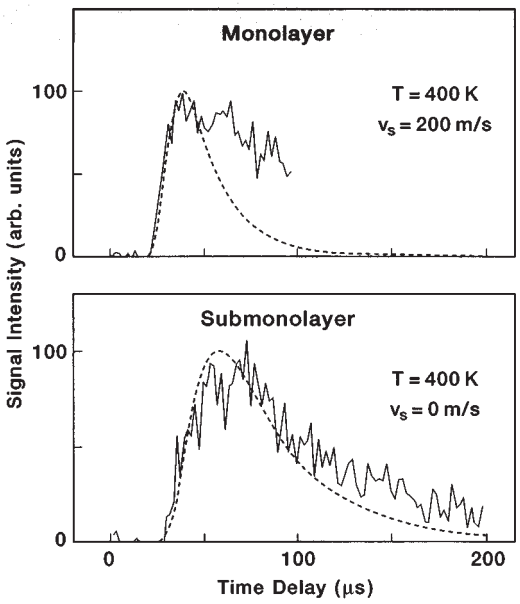


FIG. 2. TOF profiles of desorbed aniline-*d*7. Submonolayer coverages correspond to a Maxwell–Boltzmann distribution with a temperature of 400 K. Monolayer coverages correspond to a Maxwell–Boltzmann distribution with a stream velocity of 200 m/s and a temperature of 400 K. The stream velocity accounts for collisions between desorbing molecules that increase the net speed of the distribution in the direction of the surface normal.

different wavelengths are similar, except that signal intensity of the profile is larger for the distributions performed using the $O_0^0$ transition for ionization. This finding is consistent with the ion signal intensity being larger at this wavelength. Smooth self-similar profiles are obtained for both wavelengths.

The two coverages, however, result in very different distributions. The TOF profiles for monolayer and submonolayer, coverages are shown in Fig. 2. The two distributions are plotted together to emphasize the difference between them: Aniline-*d*7 molecules desorbed from monolayer coverages reach the ionization region sooner than those desorbed from submonolayer coverages. In addition, the monolayer TOF profiles exhibit trailing edges at longer times (smaller velocities) that are attributed to reflections from the electrodes and/or sample mounting assembly. Molecules traveling forward can be distinguished from those reflected backward by lowering the acceleration voltage;[34] however, we were unable to maintain acceptably high mass resolution using lower acceleration voltages.

For both monolayer and submonolayer coverages each ir laser pulse removed at least 90% of the aniline from the area irradiated by the laser pulse. When the surface rotation is interrupted, a second laser pulse applied to the same spot desorbs less than one-tenth the signal of the first laser pulse. Because nearly complete desorption occurs with each laser pulse, the temperature of desorption is justly below the maximum surface temperature of 1000 K.[35]

The widths of the profiles for both coverages are large, and some reproducible structure appears between the peaks of both profiles. The dip near the peak of the profiles is consistently found in our TOF profiles. The double-humped feature is most likely a reflection of neutral molecules returning to the ionization region. For the submonolayer coverage, the second hump in the peak of the profile corresponds with a reflection from the plate that separates the extraction region of the source from the acceleration region. The hole in this plate is small to restrict the throughput of non-normal angular components and a reflection possibly occurs from this surface. It is unlikely that the fast components in the monolayer coverages result from the added energy of a barrier because similar fast components are not observed in the submonolayer profiles. The fast components most likely result from collisional effects.

In our experiments, the ionization laser pulse is used to profile the plume of desorbed neutrals at a fixed distance, *d*, from the surface. Because the laser pulse creates ions as a function of density per unit time, rather than density per unit velocity, the Maxwell–Boltzmann time distribution is represented by the following equation.[24]

$$g(t)=C\left(\frac{1}{t^4}\right)\exp\left(-\frac{md^2}{2kTt^2}\right), \tag{1}$$

where $C$ is a constant, $t$ is the time delay between the laser desorption pulse and the ionization laser pulse, $m$ is the mass of the desorbate molecule, $k$ is the Boltzmann constant, and $T$ is the temperature of the surface when desorption occurs. The Maxwell–Boltzmann distribution function should also include an angular dependence; however, because we are detecting only molecules with velocity components normal to the surface the angular dependence is not observed in our data. When collisions occur, the net velocity of the desorbed species increases in the direction away from the surface, and the distribution function is modified to include a stream velocity, $v_s$, to account for the speed increase; the form of this distribution is shown in the following equation:[36]

$$g(t)=C\left(\frac{1}{t^4}\right)\exp\left(-\frac{m(d-tv_s)^2}{2kTt^2}\right). \tag{2}$$

The Maxwell–Boltzmann time distributions, $g(t)$, can easily be converted into velocity distributions, $f(v)$, although it is unnecessary for our analysis of the data.

The mean temperature of the desorbing aniline molecules can be estimated by comparing Maxwell–Boltzmann distributions to the TOF profiles. For these comparisons, the leading edges of the profiles (small delay times) contain the most information. The tailing edges are augmented by reflections of neutral molecules and limitations in pumping speed; molecules that take a long time to reach the ionization region do not exclusively originate from direct surface desorption.

The submonolayer profile is in agreement with a Maxwell–Boltzmann distribution at a temperature of 400 K calculated from Eq. (1) [see Fig. 2(a)]. In a microscopically reversible system, the temperature of the aniline molecules is the same as the surface from which it came. The surface temperature at the time of desorption is therefore estimated to be 400 K. The Gaussian profile of the ir laser pulse creates a temperature gradient across the desorption spot whereby

the center experiences a faster heating rate than the periphery; however, the mean temperature of the surface at the time that aniline desorbs is estimated to be 400 K.

The monolayer profile closely resembles a Maxwell–Boltzmann distribution modified with a stream velocity of 200 m/s at a temperature of 400 K calculated from Eq. (2) [see Fig. 2(b)]. Maxwell–Boltzmann distributions including a stream velocity have been used previously to describe laser desorption experiments[36] and are frequently used to describe systems in which collisions play a dominant role.[37] Another interesting feature of the monolayer profile is that a second Maxwell–Boltzmann distribution (with the same velocities and temperature $T$ but larger $d$) approximates the first hump after the leading edge. This behavior lends further support to the argument that the double-humped structure results from reflection.

### C. Vibrational assignment

The spectroscopy of aniline in its $S_0$ and $S_1$[9,10,12,13,17,38,39] state has been studied in detail, and much is known about the vibrational modes of this molecule. In particular, the geometry of aniline with respect to inversion at the nitrogen atom has been the focus of many studies. It has been firmly established that aniline is nonplanar in the ground state, whereas the excited $S_1$ state is essentially planar.[9,39]

The transition from a vibrational level, $\nu''$, in the ground electronic state to a vibrational level, $\nu'$, in the excited electronic state is represented as $K_{\nu''}^{\nu'}$ where $K$ is the normal mode. For example, the origin transition, $O_0^0$, occurs when the laser is tuned to the wavelength that excites the molecule from the $\nu''=0$ level of the ground state to the $\nu'=0$ level of the excited state. A second photon takes the molecule into the ionization continuum, and the probability for absorption of the second photon is higher than that of the first photon. For aniline, the absorption cross section for the second photon is four times larger than the absorption cross section for the first photon.[11] The ion signal generated by the two-photon transition therefore contains valuable information about the absorption of the first photon. Survey REMPI spectra of aniline-$d7$ near the origin show several strong transitions on top of a nonresonant background. Ion signal is generated at all wavelengths owing to the high density of rotational states; however, resonant transitions from the bandheads are strongly pronounced. The origin for the $S_1-S_0(^1B_2-^1A_1)$ transition for aniline-$d7$ is 292.39 nm.[9] A study of the dependence of ionization laser power on ion signal indicated that a linear relationship exists for pulse energies up to 2.5 mJ/pulse.

The first transition on the red side (longer wavelength) of the origin, $T_1^1$, has been assigned to $15b_1^1$,[12] $I_2^0 16a_0^2$,[10,13] and $10b_1^1$,[12,13] where the vibrational numbering scheme is based on the Wilson notation for benzene.[12] Although ambiguities exist in the assignment of this peak, we assign this peak in aniline exclusively to $10b_1^1$, which can be described as flexing of the amino group and the carbon skeleton of the ring. Our assignment can be rationalized as follows: (a) On the basis of single-vibronic-level fluorescence (SVLF) spectra following excitation into each of the two components of the $0_0^0+352$ cm$^{-1}$ feature it was shown[38,39] that the high and low wave number components can be assigned to $16_0^2$ and $10b_0^2$, respectively. (b) SVFL spectra following irradiation in the $T_2^2$ band[10] show identical intensities to the $10b_2^2$ bands, including the relatively weak cross-sequence bands, confirming the $10b_2^2$ assignment for this feature. (c) We have compared the intensities of $0_0^0$, $T_1^1$, and $T_2^2$ taken from gas-phase spectra[9,10,17,18,19] at room temperature, see Sec. IV D. The ratio of population in these states closely follows a thermal distribution with $T=290$ K, $E(T_1)\approx 220$ cm$^{-1}$ and $E(T_2)\approx 440$ cm$^{-1}$. Using this evidence we assign the ''$0_0^0+40$ cm$^{-1}$,'' feature[9] as $10b_1^1$ and the ''$0_0^0+80$ cm$^{-1}$,'' feature,[9] also ''$(T_2^2)$'' [10] as $10b_2^2$. Aniline-$d7$ shows a strong $10b_1^1$ feature at ''$0_0^0+45$ cm$^{-1}$,'' and a weaker $10b_2^2$ band at ''$0_0^0+90$ cm$^{-1}$,''.[10] Using these assignments and assuming the $10b$ vibrations to be harmonic in both the $\tilde{X}\ ^1A_1$ and the $\tilde{A}\ ^1B_2$ state we obtain: $\upsilon''(10b)=(217\pm 3)$ cm$^{-1}$ and $\upsilon'(10b)=(177\pm 3)$ cm$^{-1}$ for aniline-$h7$; and $\upsilon''(10b)=(203\pm 3)$ cm$^{-1}$ and $\upsilon'(10b)=(159\pm 3)$ cm$^{-1}$ for aniline-$d7$.

### D. Vibrational energy distributions

The evaluation of vibrational temperature involves the comparison of at least two $\nu'-\nu''$ vibronic bands. The following treatment, similar to one used to determine vibrational temperatures from laser-induced fluorescence experiments,[40] provides a method for deriving the populations of the two vibrational levels in the ground electronic state, $N(\nu''=0)$ and $N(\nu''=1)$.

The intensity for the absorption of the first photon, $I(\nu',\nu'')$, or the ion signal, $I$, can be written as

$$I(\nu',\nu'')=I=N(\nu'')I_L(\lambda)I_A(\nu',\nu''), \tag{3}$$

where $I_L(\lambda)$ is the laser intensity at the absorption wavelength and $I_A(\nu',\nu'')$ is the transition strength. Consider the two states, $|i\rangle$ and $|j\rangle$ with energies $E_i$ and 0, respectively. The populations for these two states can then be written as

$$N_i(\nu'')=\frac{I_i}{K_i}, \tag{4}$$

where the laser intensity and transition strength are treated as a constant $K_i$. The ratio of populations for the two states can then be described by Boltzmann statistics for a given temperature $T_x$ as

$$\frac{N_i(T_x)}{N_j(T_x)}=\exp\left(\frac{-E_i}{kT_x}\right). \tag{5}$$

Because the laser intensity and transition strength are both independent of temperature, a measurement of ion signal for two transitions, $I_i$ and $I_j$, at two temperatures, $T_1$ and $T_2$, can be described by Eqs. (4) and (5) to give

$$\ln\left(\frac{I_i(T_1)}{I_j(T_1)}\Big/\frac{I_i(T_2)}{I_j(T_2)}\right)=\frac{E_i}{k}\left(\frac{1}{T_2}-\frac{1}{T_1}\right). \tag{6}$$

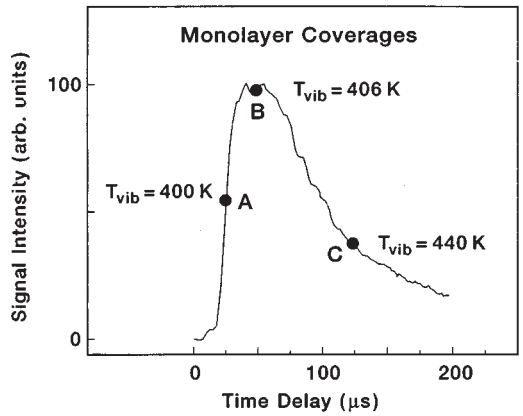


FIG. 3. Vibrational temperatures of desorbed aniline-*d*7. Vibrational temperatures are recorded at three points along a profile from monolayer coverage: A, B, and C. Similar temperature values are observed for the three points, demonstrating that collisions between desorbing molecules do not affect (i.e., cool) the vibrational energy distributions.

If the energy value $E_i$ is known and a calibration is performed at temperature $T_1$ to determine $I_i(T_1)$ and $I_j(T_1)$, then the temperature $T_2$ can be determined for molecules of unknown temperature. States with small $E_i$, such as the inversion mode of aniline ($I_1, E_i = 41\ \mathrm{cm}^{-1}$), are surely populated at room temperature, but are poor candidates for measuring the vibrational temperature of ''warm'' species (ambient temperatures) because the ratio of ion signal intensities ($I_i/I_j$) does not vary significantly for temperatures greater than 200 K. The best states for detecting warm molecules have $E_i$ values ranging between 200–500 $\mathrm{cm}^{-1}$. The $10b_1$ state of aniline-*d*7 (203 $\mathrm{cm}^{-1}$) is an excellent state for measuring the vibrational temperature, and the $10b_1^1$ transition shows a strong transition in the REMPI spectrum of aniline-*d*7.

The first information about vibrational temperatures is found from the observation that the TOF profiles taken for the two transitions are very similar. In fact, a ratio of the two profiles gives us a rough idea of vibrational temperature variations across the profile. Spectra are taken at three different laser delay times as indicated in Fig. 3. They are chosen before (A), close to (B), and shortly after (C) the maximum of the velocity distribution, thus minimizing contributions from aniline backscattered within the detection region. Then, vibrational temperatures of aniline-*d*7 desorbed from a sapphire surface are determined by comparing the population of aniline-*d*7 molecules in the $10b_1$ level ($E_i = 203\ \mathrm{cm}^{-1}$) with that in the ground state. The measurement is made indirectly using Eq. (6) with the integrated ion signals recorded for the $O_0^0$ transition (292.39 nm REMPI) and the $10b_1^1$ transition (292.77 nm REMPI) for aniline-*d*7 backfilled into the chamber ($T_1 = 290$ K) and aniline-*d*7 desorbed from the sapphire surface with a fixed time delay between desorption and ionization pulses. The calibration is performed by recording an averaged mass spectrum for the each transition and integrating the ion signal for aniline-*d*7. The integrated values are placed directly into Eq. (6) without further treatment because we found in our calibration studies that this method was acceptable. For aniline desorbed from the surface, a time delay between laser pulses is fixed and two-step and gas-phase background mass spectra are acquired alternately at 5 Hz for both REMPI transitions. We record these averaged mass spectra, integrate the aniline-*d*7 peaks, and place the integrated values into Eq. (6). We find the ratio of the $10b_1^1$ TOF profile to the $O_0^0$ TOF profile to be nearly constant over the profile, indicating that the temperature is uniform for all times of the profile.

Spectra are taken at three different laser delay times as indicated in Fig. 3. Vibrational temperature analyses performed on three regions of the profile [A (25 $\mu$s), B (50 $\mu$s), and C (125 $\mu$s)] all yield similar values. The ratio of the $10b_1^1$ value to the $O_0^0$ value for A ($0.87 \pm 0.13$), B ($0.88 \pm 0.08$), and C ($0.93 \pm 0.10$) are all consistent with each other and larger than the gas-phase calibration ratio at 290 K ($0.66 \pm 0.11$). The latter one is within 10% of the ratio of the integrated areas of the two bands in the gas-phase spectrum. The desorbed aniline molecules are clearly warmer than 290 K, and the mean value for the temperatures of the three points on the distribution is found to be 415 K. The error associated with converting ratios into temperatures is nonlinear. The ratio values with one sigma error bars translate into a temperature range of 350–550 K.

## V. DISCUSSION

The agreement between the translational temperature and the internal temperature supports a model of aniline-*d*7 leaving the sapphire surface in full equilibrium between translational and internal energy of this molecule, and presumably with the surface at the time the molecule escapes. The results presented here indicate that pulsed laser-induced desorption from insulator surfaces occurs via a thermal mechanism, that is molecules desorb from the surface in such a manner that translational and vibrational temperatures are equilibrated. We conclude that there is no bottleneck to the energy flow in the desorption process, because the energy of the adbond (exhibited in the translational energy distribution) follows the temperature of the surface at the time of desorption.

We tested for isotopic selectivity in the desorption process by detecting aniline-*d*7 simultaneously with aniline-*d*6 ($C_6D_5NHD$) and aniline-*d*5 ($C_6D_5NH_2$). The three isotope combinations are created in the gas reservoir and the gas inlet line and dosed through the glass multicapillary array. After correcting for their different concentrations, measured in the ''gas-phase'' mode, our two-step desorption experiments verified that no selective desorption was observed for both submonolayer and monolayer of isotopically mixed aniline on sapphire. Nearly equal amounts of the three different isotope combinations were observed to desorb from the surface showing within error the same translational and vibrational distribution. The desorption yields are also similar for aniline-*h*7, i.e., for the purely protonated aniline at equivalent coverages; although, quantitative comparison is difficult owing to different dye mixtures and wavelength regions used for detection.

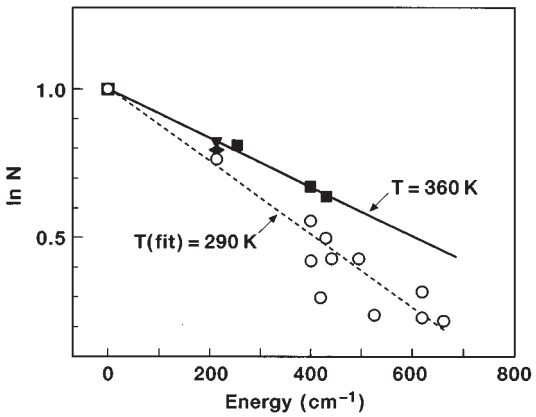


FIG. 4. Comparison of vibrational temperatures of desorbed aniline. Vibrational distributions versus energy for (1) a monolayer of aniline-*h*7 desorbed from a quartz surface (Ref. 17) triangle, (2) 0.01 ML of aniline-*h*7 desorbed from the same surface (Ref. 18) diamond, (3) aniline-*h*7 evaporated from a $CO_2$ matrix (Ref. 19) squares. Similar temperature values are observed for the three different experiments, demonstrating that collisions between desorbing molecules do not affect (i.e., cool) the vibrational energy distributions. Intensity analysis of different hot vibrational bands in the different spectra give similar vibrational temperatures of ~360 K. The dotted line and the superimposed open circles belong to room-temperature ($T \sim 290$ K) calibration spectra of aniline in the gas phase (static cell, $10^{-3}$ Torr) taken at different laboratories (Refs. 9, 10, 17, and 19).

Our experimental results for translational and internal energy distributions of aniline desorbing from sapphire are similar to those of Voumard *et al.*[17,18] for aniline desorbing from quartz, but the interpretation differs. Although not reported together, Voumard *et al.* find submonolayers of aniline on quartz desorb with a mean translational energy of 350 K,[17] a mean vibrational temperature of 360 K,[18] and a mean rotational temperature of 350 K.[18] Although their data are consistent with our description of an equilibrium process, they contend that the temperature of the surface at the time of desorption is not equivalent to a translational energy distribution but rather can be extrapolated from kinetic parameters derived from temperature programmed desorption. They calculate a surface temperature of 500 to 600 K at the time of desorption which supports a desorption mechanism dominated by a bottleneck for energy flow after rapid heating of the surface (at about $10^9$ K/s). We do not observe molecules leaving the surface with temperatures (translational) this large, and we estimate a lesser surface temperature; however, we recognize that neither Voumard *et al.*[17,18] nor this study directly measured the temperature of the surface at the time of desorption. Consequently, more experiments are needed to settle this question in a definitive manner.

Because the assignment of the $T_1^1$ state was previously ambiguous, we have reanalyzed the work of Elokhin *et al.*,[19] and find that collisional cooling does not occur, even for mixtures of aniline with an excess of $CO_2$. Using several transitions, *except* the $10b_1^1$ transition, to determine the vibrational temperature of the desorbing aniline, we find that the internal energy of the desorbing species is far larger than the value they report. Figure 4 collects the results of overall desorption measurements of aniline made in different laboratories using similar (insulator) surfaces and laser-induced rapid heating. We analyzed the published spectra to gain insight into the vibrational energy distributions of aniline. The results consist of (1) band peak heights for different vibronic levels measured with (1+1) REMPI and different coverages of aniline-*h*7,[17,18] (2) band areas for different vibronic levels measured with (1+1) REMPI and submonolayers of aniline-*h*7,[18] and (3) aniline-*h*7 evaporated from a $CO_2$ matrix using the first harmonic of a Nd:YAG laser and (1+1) REMPI detection.[19] A least squares fit to the measured distributions (1) to (3) is also shown.

Several comments concerning Fig. 4 are pertinent here. The first is that the values of $T$ agree reasonably well with the ''collision-free'' monolayer measurements by other laboratories[17,18] and the results presented here. Second, we note that even at many layers including additional $CO_2$ coverage[19] the vibrational energy distributions are not altered dramatically.

All these data taken under quite different experimental condition lead us to conclude that rapid thermalization of the desorbed molecules is the main channel for laser-induced desorption at the heating rates studied to date. Moreover, it is also reasonable to suppose that translational and vibrational energy distributions are governed by the same temperature, so long as post-desorption collisions do not alter this behavior.

The question remains under what conditions will selective LD occur for molecules on dielectric surfaces. Clearly more experiments are needed, particularly those conducted at faster heating rates and weaker surface–adsorbate interactions.

[1] R. B. Hall, J. Phys. Chem. **91**, 1007 (1987).
[2] *Laser Ionization Mass Analysis*, edited by A. Vertes, R. Gijbels, and F. Adams (Wiley, New York, 1993).
[3] A. Overberg, M. Karas, U. Bahr, R. Kaufmann, and F. Hillenkamp, Rapid Commun. Mass Spectrom. **4**, 293 (1990).
[4] T. J. Chuang, H. Seki, and I. Hussla, Surf. Sci. **158**, 525 (1985).
[5] T. J. Chuang, Surf. Sci. Rep. **3**, 1 (1983).
[6] J. Heidberg and D. Hoge, J. Opt. Soc. Am. B **4**, 242 (1987).
[7] M. Buck and P. Hess, Chem. Phys. Lett. **158**, 486 (1989).
[8] F. Budde, A. V. Hamza, P. M. Ferm, G. Ertl, D. Weide, P. Andresen, and H.-J. Freund, Phys. Rev. Lett. **60**, 1518 (1988); K. Fukutani, Y. Murata, R. Scwarzwald, and T. J. Chuang, Surf. Sci. **311**, 247 (1994); W. C. Natzle, D. Padowitz, and S. J. Sibener, J. Chem. Phys. **88**, 7975 (1988); F. Hillenkamp, M. Karas, D. Holtkamp, and P. Klusener, Int. J. Mass Spectrom. Ion Proc. **69**, 256 (1986); S. J. Clemett, A. W. Parker, K. von Puttkamer, A. Takami, and C. J. S. M. Simpson, J. Electr. Spectrosc. **54**,**55**, 211 (1990).
[9] J. C. D. Brand, D. R. Williams, and T. J. Cook, J. Mol. Spectrosc. **20**, 359 (1966).
[10] D. A. Chernoff and S. A. Rice, J. Chem. Phys. **70**, 2511 (1979).
[11] J. H. Brophy and C. T. Rettner, Chem. Phys. Lett. **67**, 351 (1979); C. T. Rettner and J. H. Brophy, Chem. Phys. **56**, 53 (1981).
[12] G. Varsanyi, *Assignments for Vibrational Spectra of Seven Hundred Benzene Derivatives* (Wiley, New York, 1974).
[13] R. Scheps, D. Florida, and S. A. Rice, J. Chem. Phys. **61**, 1730 (1974).
[14] B. Hader and O. Weis, Surf. Sci. **220**, 118 (1989).
[15] J. B. Peri, J. Phys. Chem. **69**, 220 (1965).
[16] A. Vertes and R. Gijbels, in *Laser Ionization Mass Analysis*, edited by A. Vertes, R. Gijbels, and F. Adams (Wiley, New York, 1993), pp. 127–176.
[17] P. Voumard, R. Zenobi, and Q. Zhan, Surf. Sci. **307–309**, 360 (1994).
[18] P. Voumard, R. Zenobi, and Q. Zhan, J. Phys. Chem. **99**, 11 722 (1995).

[19] V. A. Elokhin, A. N. Krutchinsky, and S. E. Ryabov, Chem. Phys. Lett. **170**, 193 (1990).
[20] P. A. Redhead, Vacuum **12**, 203 (1962).
[21] R. J. Beuhler and L. Friedman, Int. J. Mass Spectrom. Ion Proc. **78**, 1 (1987).
[22] R. Kelley and R. W. Dreyfus, Nucl. Instr. Meth. Phys. Res. B **32**, 341 (1988).
[23] I. NoorBatcha, R. R. Lucchese, and Y. Zeiri, J. Chem. Phys. **86**, 5816 (1987).
[24] M. Asscher, F. M. Zimmermann, L. L. Springsteen, P. L. Houston, and W. Ho, J. Chem. Phys. **96**, 4808 (1992).
[25] R. N. Zare and R. D. Levine, Chem. Phys. Lett. **136**, 593 (1987).
[26] T. A. Holme and R. D. Levine, Surf. Sci. **216**, 587 (1989).
[27] R. R. Lucchese and J. C. Tully, J. Chem. Phys. **81**, 6313 (1984).
[28] C. R. Maechling, Ph.D. thesis, Stanford University, Stanford, CA, 1995.
[29] S. E. Bialkowski, Rev. Sci. Instrum. **58**, 2338 (1987).
[30] W. C. Wiley and I. H. McLaren, Rev. Sci. Instrum. **26**, 1150 (1955).
[31] R. Zenobi, J. H. Hahn, and R. N. Zare, Chem. Phys. Lett. **150**, 361 (1988).
[32] J.-M. Philippoz, R. Zenobi, and R. N. Zare, Chem. Phys. Lett. **158**, 12 (1989).
[33] *Thermophysical Properties of Matter*, edited by Y. S. Touloukian and C. Y. Ho (Plenum, New York, 1970), Vol. 2 pp. 93–119, Vol. 5 pp. 24–29, Vol. 8 pp. 187–189.
[34] K. A. Trentelman, D. H. Fairbrother, P. G. Strupp, P. C. Stair, and E. Weitz, J. Chem. Phys. **96**, 922 (1992).
[35] D. Burgess, Jr., P. C. Stair, and E. Weitz, J. Vac. Sci. Technol. A **4**, 1362 (1986).
[36] P. Hess, in *Topics in Current Physics*, Vol. 47, edited by P. Hess (Springer, Berlin, 1989).
[37] J.-Y. Zhang, D. S. Nagra, and L. Li, Anal. Chem. **65**, 2812 (1993).
[38] E. R. Bernstein, K. Law, and M. Schauer, J. Chem. Phys. **80**, 207 (1984).
[39] A. R. Bacon and J. M. Hollas, Faraday Discuss. **86**, 129 (1988).
[40] G. M. McClelland, K. L. Saenger, J. J. Valentini, and D. R. Herschbach, J. Phys. Chem. **83**, 947 (1979).